Journal of Materials Chemistry B

ROYAL SOCIETY OF CHEMISTRY

PAPER

View Article Online
View Journal | View Issue

Cite this: *J. Mater. Chem. B*, 2021, **9**, 4502

Synthesis of maleimide-based enediynes with cyclopropane moieties for enhanced cytotoxicity under normoxic and hypoxic conditions†

Wenbo Wang, Haotian Lu, Mengsi Zhang, Hailong Ma, Xiaoyu Cheng, Yun Ding * and Aiguo Hu *

Received 22nd January 2021,
Accepted 29th April 2021

DOI: 10.1039/d1tb00142f

rsc.li/materials-b

Myers-Saito cycloaromatization (MSC) is the working mechanism of many natural enediyne antibiotics with high antitumor potency. However, the presence of the equilibrium between diradical and zwitterionic intermediates in MSC severely hinders further improvement in cytotoxicity toward tumor cells. To this end, a series of maleimide-based enediynes with cyclopropane moieties were synthesized for enhanced cytotoxicity toward tumor cells. By taking advantage of radical clock reactions, the diradical intermediates generated from MSC would rearrange to new diradicals with much longer separation and weaker interactions between two radical centers. The computational study suggested a low energy barrier (4.4 kcal mol^{-1}) for the radical rearrangement through the cyclopropane ring-opening process. Thermolysis experiments confirmed that this radical rearrangement results in the formation of a new diradical intermediate, followed by abstracting hydrogen atoms from 1, 4-cyclohexadiene. Interestingly, the DNA cleavage ability and cytotoxicity of enediynes were significantly enhanced after the introduction of cyclopropane moieties. In addition, these maleimide-based enediynes exhibited a similar cytotoxicity under hypoxic conditions to that under normoxic conditions, which is beneficial for treating solid tumors where hypoxic environments frequently lead to deteriorated efficiency of many antitumor drugs. Docking studies indicated that the diradical intermediate was located between the minor groove of DNA with a binding energy of −7.40 kcal mol^{-1}, which is in favor of intracellular DNA damage, and thereby inducing cell death *via* an apoptosis pathway as suggested by immunofluorescence analysis.

Introduction

Naturally occurring antibiotics bearing unique enediyne moieties including neocarzinostatin (NCS),[1,2] calicheamicin (CAL),[3] dynemicin (DYN),[4] and esperamicin (ESP)[5] exhibit significant inhibition effects on an array of tumor cell lines with half inhibition concentration (IC_{50}) down to the nanomolar level and have been acknowledged as the strongest chemotherapeutic agents ever discovered.[6,7] They exert excellent antitumor activity by virtue of their outstanding DNA cleavage ability, in which the highly reactive radicals formed from these enediynes can efficiently deprive hydrogen atoms from the phosphate backbone of DNA. The high bioactivity of natural enediynes is intriguing and has attracted a stream of research efforts to design and synthesize their analogues with the aim of attaining the optimal cytotoxicity for the targeted cancer therapy.[8–11]

The working mechanism of enediyne antibiotics to produce highly reactive diradical intermediates is classified either through the Bergman cyclization (BC, typically for CAL, DYN, ESP and their analogues)[12] or Myers-Saito cyclization (MSC, typically for NCS and its analogues) pathway[13] under physiological conditions. In the BC pathway, a homosymmetric σ, σ-biradical is formed, while in the MSC pathway, a heterosymmetric σ,π-biradical intermediate is formed after the thermal cycloaromatization. Unlike the high reactivity of natural enediynes to afford diradicals upon specific triggering behavior, the synthetic enediyne compounds typically face the dilemma of balancing the reactivity and stability in certain cases. Considering the much lower energy barrier of MSC in comparison with BC, converting stable enediynes to enyne-allenes (precursors for MSC) is a promising strategy for generating reactive diradicals under low temperatures[14–16] to be potentially applied for cancer chemotherapy. In the last two decades, much efforts have been dedicated to synthesizing enyne-allene compounds

Shanghai Key Laboratory of Advanced Polymeric Materials, School of Materials Science and Engineering, East China University of Science and Technology, Shanghai 200237, China. E-mail: yunding@ecust.edu.cn, hagmhsn@ecust.edu.cn

† Electronic supplementary information (ESI) available. See DOI: 10.1039/d1tb00142f

from stable enediyne precursors, followed by producing α, 3-toluene σ,π-diradical intermediates through the MSC pathway.[17–19] Unfortunately, the conditions applied for generating enyne-allenes like high temperature,[17] addition of gold complex,[18] and shining with UV light[19] are incompatible with the biological environment, limiting their further application in the treatment of cancer. Recently, our group uncovered a new mechanism, named maleimide assisted rearrangement and cycloaromatization (MARACA),[20] in which the conversion of stable acyclic enediynes to reactive enyne-allenes was greatly accelerated by employing maleimide moieties at the ene position, leading to the facile MSC pathway in a physiological environment.[20–22]

Despite many favorable factors of MSC to produce highly reactive diradicals under mild conditions, there are two noticeable issues that limit the H-abstracting ability of the diradicals formed through MSC. On one hand, the loss of one chemical bond in MSC might produce an unusual zwitterionic species rather than a diradical intermediate *via* the cycloaromatization of enyne-allenes (Scheme 1A).[16,23,24] Early studies by Myers[25] and Saito[26] proposed a zwitterionic mechanism to account for the generation of the observed products, considering the presence of an equilibrium between diradical and zwitterionic intermediates. Shibuya *et al.*[27] further confirmed that polar conditions were conducive to the formation of zwitterionic intermediates derived from the MSC pathway. On the other hand, theoretical and experimental evidences have shown that diradicals derived from enediynes could be rapidly attacked by nucleophiles to form ionic-type products owing to the close interaction between two radical centers (Scheme 1B).[28,29] Unfortunately, the presence of ionic intermediates and the increase of ionic-type products are believed to lower the extent of DNA damage, thereby reducing the therapeutic effect on cancers.[7,8,15,20]

Increasing the distance between two radical sites will decrease the spin–spin coupling between them, thereby breaking the equilibrium between diradical and zwitterionic intermediates.[30] The cyclopropane ring-opening process, which has been frequently used in radical chemistry as a radical clock,[31–35] may provide a possible way to increase the distance between two original radicals. Indeed, Finn[36] and Myers[25] have shown that cyclopropane substituted enyne-allenes produced more reactive biradicals by the ring-opening process (Schemes 1C and D), followed by faster H-abstraction from 1,4-cyclohexadiene (1,4-CHD). To this end, we herein report the design and synthesis of a series of maleimide-based enediynes carrying various cyclopropane moieties at the alkyne termini to enhance their cytotoxicity to cancer cell lines. The computational study and thermolysis experiments on the model compound showed that diradicals generated from **EDY-A** through the MARACA mechanism were prone to undergo radical clock reactions to generate a new product with *trans* double bonds after the cyclopropane ring-opening process followed by H-abstraction from 1,4-CHD. Electron paramagnetic resonance (EPR) spectroscopy and reactive oxygen species (ROS) detection experiments showed that enediynes with potential radical clock pathways had stronger ability to generate reactive radical species, and this result was also consistent with the results of DNA cleavage and cancer cell variation inhibition experiments. These maleimide-based enediynes exhibit an unaffected cytotoxicity under hypoxic conditions. Further studies indicated that the S phase of the cell cycle was arrested through intracellular DNA damage originated from enediynes, thereby inducing cell death *via* an apoptosis pathway.

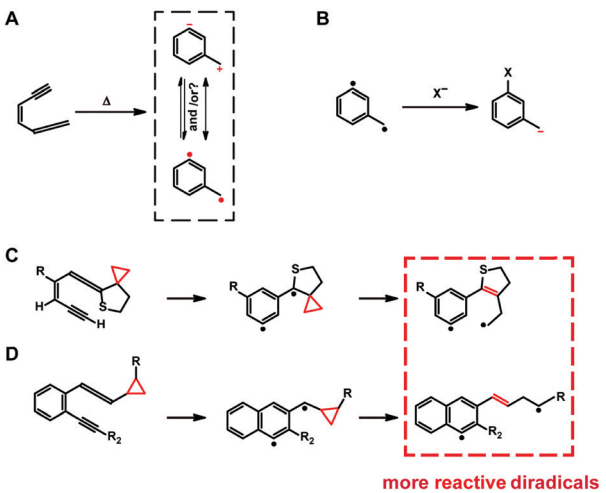

Scheme 1 (A) and (B) The formation pathways of ionic-type products in MSC reactions. Radical clock reactions in MSC reactions reported by Myers (C) and Finn (D).

Results and discussion

Design and synthesis of enediynes with radical clock moieties

Considering that maleimide-based enediynes with propargyl ester groups exhibit high cytotoxicity toward tumor cell lines[20,37] and the cyclopropane ring has been widely used in radical clock reactions, six enediynes with (substituted) propargyl ester groups were synthesized through Sonogashira cross coupling reactions between compound C3 and the corresponding terminal alkynes at room temperature (Scheme 2). Among them, three enediynes were employed with cyclopropane moieties while other three enediynes were designed with a similar structure but with no cyclopropyl substituent. The chemical structures of all these enediynes were characterized by ^{1}H NMR, ^{13}C NMR and ESI-MS spectroscopies (ESI†).

MSC Cyclization in the presence of 1,4-CHD

According to our previous work, the maleimide-based enediynes are prone to undergo MSC reactions through cascade 1,3-proton transfer and then to generate reactive radicals (MARACA), which can efficiently deprive hydrogen atoms from the environment. To gain further insight into the reaction pathway of radicals generated through the MARACA mechanism, H-abstracting experiments with 1,4-CHD as an external H-atom donor were performed with model compound **EDY-A**.[31,36,39] Briefly, a **EDY-A** solution (10 mM) in 1,4-CHD

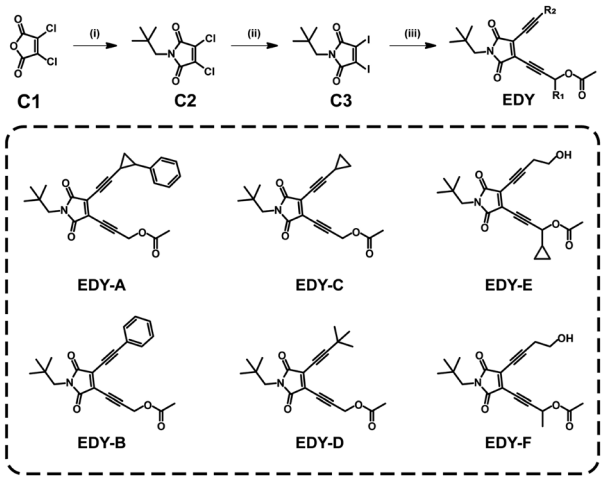

Scheme 2 Synthesis of enediyne compounds: (i) neopentylamine, acetic acid, 45 °C, 18 h. (ii) NaI, acetonitrile, 90 °C, 15 h. (iii) NHC-$PdCl_2$-3-chloropyridine, CuI, DIPEA, alkyne, toluene/THF, rt, 15 h.

was heated at 80 °C in a sealed tube in the presence of *N*, *N*-diisopropylethylamine (5 equiv.) for 96 h. It should be noted that the MARACA process is retarded in the nonpolar environment;[20] even by adding a base to facilitate the propargyl-allene tautomerization process, the reaction was sluggish at room temperature. After complete conversion of **EDY-A**, a mixture of small molecular compounds was formed, none of which could be separated out in pure form. This may be due to the presence of various intramolecular radical transfer processes, leading to the formation of diverse hydrogen abstraction products with similar polarities.[38,39] Nevertheless, the ^{1}H NMR spectrum of the mixture still provide valuable information as shown in Fig. 1B. The signals at 6.10 (^3J = 12.2 Hz, ^3J = 6.3 Hz, dt) and 6.36 ppm (^3J = 12.2 Hz, ^4J =1.9 Hz, dt) are characteristic peaks attributed to *trans* double bonds with a methylene group at one side and an aryl group at the other side.[40,41] The formation of this kind of structure is highly interesting, which indicates that **EDY-A** undergoes cascade rearrangement to generate enyne-allenes for MSC to take place (MARACA). The newly formed phenyl radical appears at the α-position of the cyclopropane group, initiating the radical clock reaction to generate a *trans* double bond and to separate two radical sites faraway. Due to the reduction of the interaction between two free radicals,[30] the H-abstraction from 1,4-CHD is greatly facilitated to generate a stable compound (Fig. 1A). The high resolution mass spectrum (Fig. S1, ESI†) shows a peak with *m*/*z* of 428.1837, corresponding to this H-abstraction product.

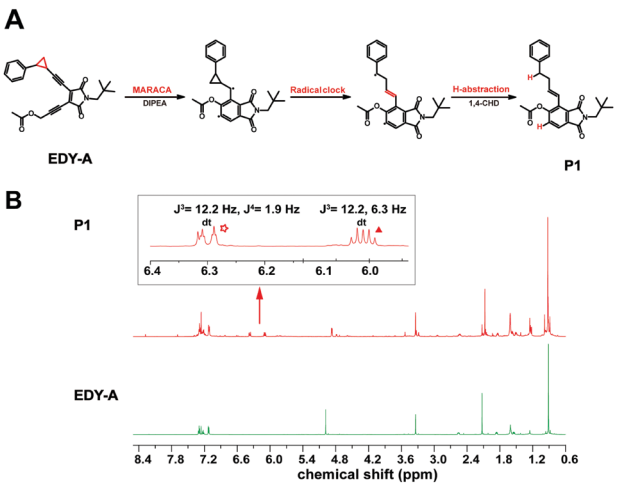

Fig. 1 (A) MARACA and possible radical clock pathway of **EDY-A** in the presence of 1,4-CHD. (B) Comparison of the ^{1}H NMR spectra of **EDY-A** and cyclization products containing P1.

Computational study

To further understand the possibility of radical clock reactions and the reactivity of the newly generated diradicals, a standard density functional theory (DFT) method (B3LYP) in combination with a 6-31G(d) basis set was selected for the in-depth investigation of the potential reaction pathways leading to the observed products. Our previous work has demonstrated that maleimide-based enediynes can generate reactive diradicals through the MARACA mechanism,[20] therefore, only the radical clock reaction pathway and the pathway for radicals abstracting hydrogen from 1,4-CHD were calculated in this work. The calculation of harmonic vibration frequency was carried out at 298.15 K, 1 atm and the optimization of structures was all displayed to be either minima (with no imaginary frequency) or transition states (with only 1 imaginary frequency). Intrinsic reaction coordinate calculations provide further evidence that each **TS** serves as a linker between the corresponding reactants and products. As shown in Fig. 2, the calculated energy barrier for cyclopropane ring opening of diradicals **H1** to **H2** is about 4.4 kcal mol^{-1}, which is relatively low, and the energy barrier of the newly generated diradicals to abstract hydrogen from 1, 4-CHD is 13.1 kcal mol^{-1}. According to the experimental and computational results, the diradicals generated through the MARACA mechanism are prone to transfer into diradicals separated by a longer distance through rapid radical clock

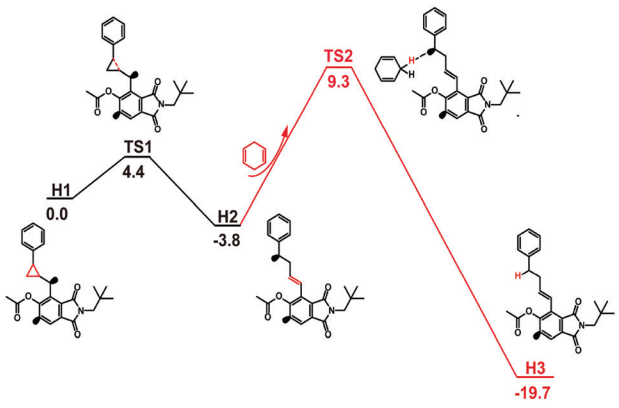

Fig. 2 The calculated Gibbs free energies (kcal mol^{-1}) along the reaction pathway of the diradical product of **EDY-A**. Black lines for radical clock reactions with the designed ring-opening process, and red lines for H-abstraction using 1,4-CHD as an external H-atom donor.

reactions, thereby decreasing the interaction of the biradical species and enhancing their radical character for the subsequent radical abstracting reactions.

Detection of radical intermediates

Electron paramagnetic resonance (EPR) experiments were carried out to prove the generation of active free radicals from the newly designed enediynes.[42] Due to the difficulty of monitoring active carbon radicals, a spin-trap agent, phenyl *tert*-butyl nitrone (PBN), was employed to convert the active carbon radicals into stable nitroxide free radicals for EPR analysis. All enediynes (20 mM) were respectively incubated with excessive PBN (100 mM) in 1,2-dichloroethane (DCE) at 37 °C for 12 h and then subjected to EPR experiments. As shown in Fig. 3A, a typical triplet peak at 3520 G corresponding to nitroxide free radicals suggested that **EDY-A** had undergone a cycloaromatization reaction to generate radicals at this low temperature. Other kinds of enediynes showed similar EPR spectra as shown in Fig. S2 (ESI†). In addition, the generation of diradicals of two model compounds in the polar environment was evaluated using 1,3-diphenylisobenzofuran (DPBF) as an indicator, whose absorption at 416 nm in DMSO solution is quenched by $^1O_2$ induced by diradicals.[43] As shown in Fig. 3B, the absorbance of DPBF in DMSO solution gradually decreased at 37 °C with prolonged time, and the absorbance of DPBF treated with **EDY-A** decayed much faster in comparison with that treated with **EDY-B**, suggesting that **EDY-A** generated more reactive free radicals under identical conditions. The ability of enediynes to produce highly reactive radicals endows them with high potential for DNA-cleavage and tumor cell variation inhibition.

Evaluation of the DNA-cleavage ability of enediynes

DNA agarose gel electrophoresis was exploited to perform in-depth investigation on the DNA-cleavage ability of enediynes. Negatively supercoiled pUC19 plasmid DNA was cultured with enediynes at 37 °C for 48 h in 50% (v/v) DMSO before being subjected to electrophoresis. As shown in Fig. 3C and E, all enediynes were highly efficient for DNA cleavage, and among them, **EDY-E** led to complete DNA cleavage from Form I (supercoil) to Form II (cyclic) at the same concentration. Interestingly, enediynes with cyclopropane moieties generally showed stronger DNA cleavage ability probably due to the existence of the radical clock reaction pathway to enhance the character of the diradical species. The DNA-cleavage of enediynes was also concentration-dependent (Fig. 3D). Taking **EDY-E** as an example, increasing the concentration of enediyne caused the decrease of pristine form I of pUC19, accompanied by the increase of form II. At a concentration of 15 mM, DNA was completely cut into low molecular weight fragments.

Evaluation of the cytotoxicity of enediynes

The 3-(4,5-dimethyl-2-thiazolyl)-2,5-diphenyl-2Htetrazolium bromide (MTT) assay was employed to assess the cytotoxicity of various enediynes to HeLa cell lines. As shown in Fig. 3F, IC_{50} values down to 2.0 μM was achieved with these enediynes, comparable to many commercial antitumor agents.[44–46]

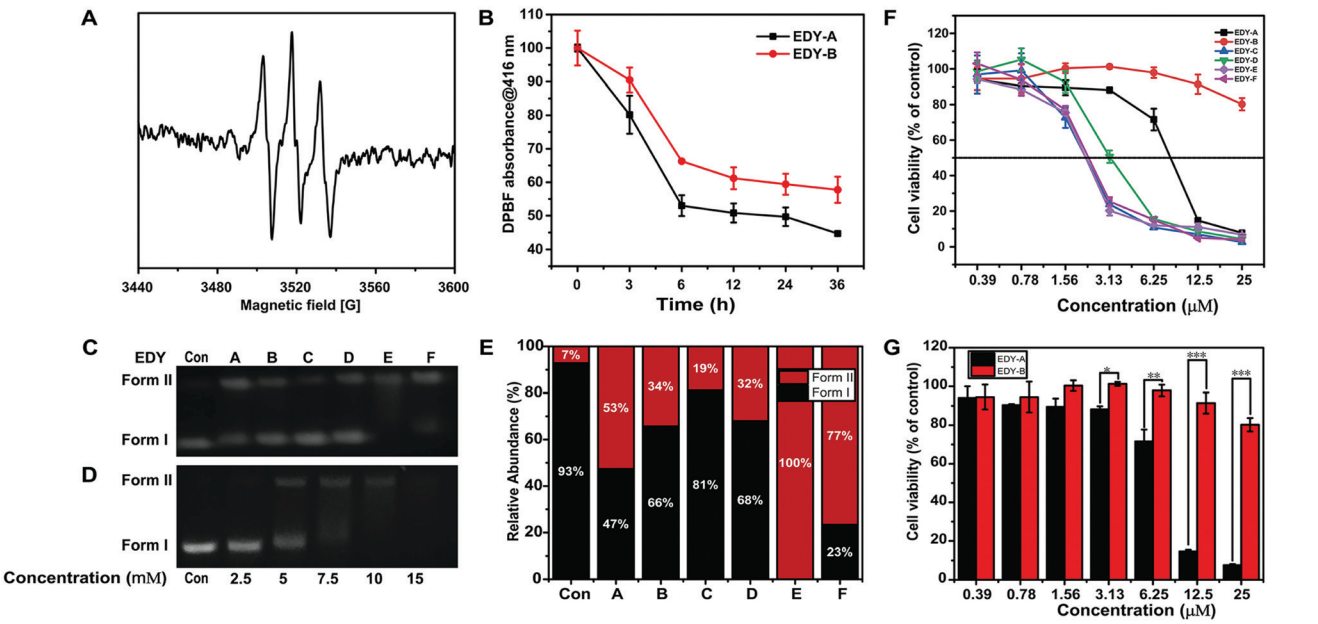

Fig. 3 (A) EPR spectrum of **EDY-A** (20 mM) in DCE after heating at 37 °C for 12 h in the presence of PBN (100 mM). (B) The absorbance of DPBF at 416 nm in the presence of **EDY-A** (black line) and **EDY-B** (red line). (C) and (E) Agarose gel electrophoretic image of six enediynes and quantified cleavage data for DNA cleavage assay. Control: pUC19 (10 μg ml^{-1}) alone; A to F: pUC19 (10 μg ml^{-1}) incubated with 10 mM of the corresponding enediynes. (D) Agarose gel electrophoretic image for DNA cleavage by 0, 2.5, 5.0, 7.5, 10, and 15 mM of **EDY-E** at 37 °C for 48 h. Code: intact DNA (Form I, black block), single-strand scission (Form II, red block). (F) The cytotoxicity of enediynes against HeLa cells determined by the MTT assay. (G) Comparison of the cytotoxicity of **EDY-A** and **EDY-B**.

The enediynes with cyclopropane moieties typically showed higher cytotoxicity, similar to the results in DNA-cleavage experiments. In particular, the cytotoxicity of **EDY-A** (IC_{50} = 7.90 μM) is significantly higher than that of **EDY-B** (IC_{50} > 25 μM) with a similar structure and logP values (4.17 *vs* 3.92) as shown in Fig. 3G. Similar cytotoxic performance of the maleimide-based enediynes was observed in other three types of cancer cell lines (Fig. S3, ESI†). Overall, this radical clock strategy may provide a promising way to promote the synthesis of robust maleimide-based enediyne compounds for antitumor applications.

Compared to normal cells, cancer cells in solid tumors have a much faster rate of metabolism and proliferation, causing cancer cells to have faster oxygen consumption rate, and the tumor microenvironment tends to be hypoxic. It has been confirmed that the tumor hypoxia microenvironment enhances the resistance of cancer cells to a variety of antitumor agents by different ways.[47–49] Therefore, it is of essential importance to develop chemotherapeutic agents that maintain excellent cytotoxicity under hypoxic conditions. To test the cytotoxicity of enediynes under hypoxic conditions, deferoxamine (DFO), a typical hypoxia inducer, was employed with HeLa cells for this experiment. As shown in Fig. 4 and Fig. S4 (ESI†), notably, when HeLa cells were incubated with DFO (200 μM) for 12 h, at this concentration, the hypoxia environment can be significantly produced,[50] and negligible cytotoxicity is observed. Fig. 4 also shows that the groups treated with **EDY-E** only (12.5 μM) and **EDY-E** (12.5 μM) together with DFO (200 μM) exhibit similar cytotoxicity, suggesting that the cytotoxicity under anaerobic conditions is mainly contributed by carbon free radicals rather than ROS induced by enediyne. This oxygen-independent character of maleimide-based enediyne provides a possibility for their application in chemotherapy for solid tumors.

Cellular uptake and intracellular radical generation of enediynes

The entry of enediyne molecules into the nuclei is a prerequisite for its DNA cleavage ability to be revealed. Benefiting from the inherent fluorescence of enediynes (Fig. S5, ESI†), it is convenient for us to assess the cellular internalization *in situ* using a confocal laser scanning microscope (CLSM).[51] HeLa cells were incubated with **EDY-E** or **EDY-F** for 8 h, and then stained with propidium iodide (PI, red) to locate the nucleus. As illustrated in Fig. 5A, the overlap of bright blue fluorescence of enediyne and red fluorescence of PI (nucleus) is observed, indicating the effective entry of **EDY-E** and **EDY-F** into the nucleus. Afterwards, 2′,7′-dichlorofluorescin diacetate (DCFH-DA), a cell-permeable ROS indicator,[51] was utilized for detecting intracellular free radicals. Upon intracellular hydrolysis and reaction with free radicals, DCFH-DA can be rapidly converted into a green fluorescent molecule (2′,7′-dichlorodihydrofluorescein, DCF). As shown in Fig. 5B, compared to the control groups without addition of enediyne, the significantly enhanced green fluorescence intensity induced by **EDY-E** or **EDY-F** was observed inside the cells by using a CLSM, confirming the effective generation of reactive free radicals by enediyne in cells, causing cell death after radical induced DNA cleavage.

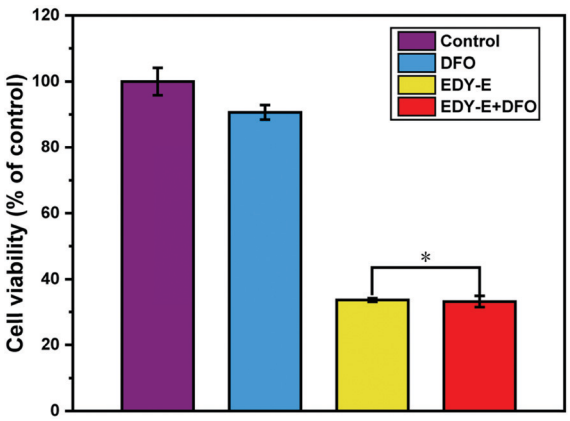

Fig. 4 The cytotoxicity of enediynes against HeLa cells under normoxic and hypoxic conditions.

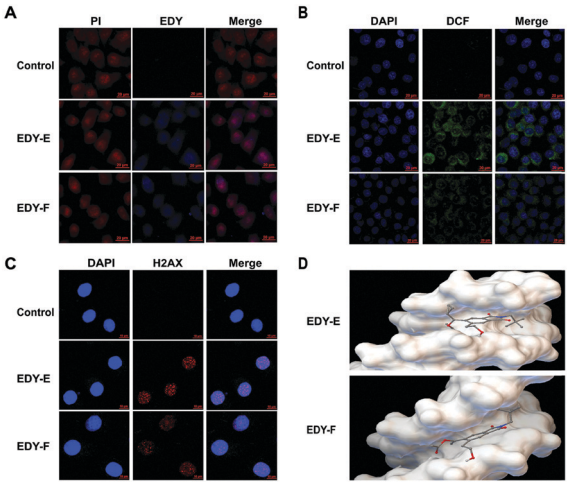

Fig. 5 (A) Cellular uptake of **EDY-E** and **EDY-F** (1 μM), (B) Intracellular free radical detection for **EDY-E** and **EDY-F** (1 μM). (C) Intracellular DNA damage (H2AX as an indicator, red) induced by **EDY-E** and **EDY-F**. (D) Molecular models for diradicals generated from **EDY-E** and **EDY-F** docked into the minor groove of DNA. The images are of the most favorable conformations.

Docking studies and DNA damage detection in HeLa Cells.

Docking studies[52–54] are often used to evaluate the interaction of drug molecules with DNA, which were performed on the diradical intermediates formed from **EDY-E** and **EDY-F**. The free binding energy of **EDY-E** or **EDY-F** with ct-DNA (PDB ID:453D) calculated through Autodock4.2[55] was −7.40 kcal mol^{-1} and −7.25 kcal mol^{-1} (Fig. S6, ESI†). The negative binding values for **EDY** indicate that the binding of DNA and diradical intermediates is thermodynamically favorable. As can be seen in Fig. 5D, diradical intermediates generated through MARACA reactions are located parallel to the groove walls of the selected ct-DNA. This orientation can further help the diradical intermediates to proceed to intercalate between base pairs, thereby improving the ability to cleave DNA.[54,56] To gain in-depth insight into the toxigenic effect of radicals generated from enediynes, immunofluorescence analysis was conducted to detect the

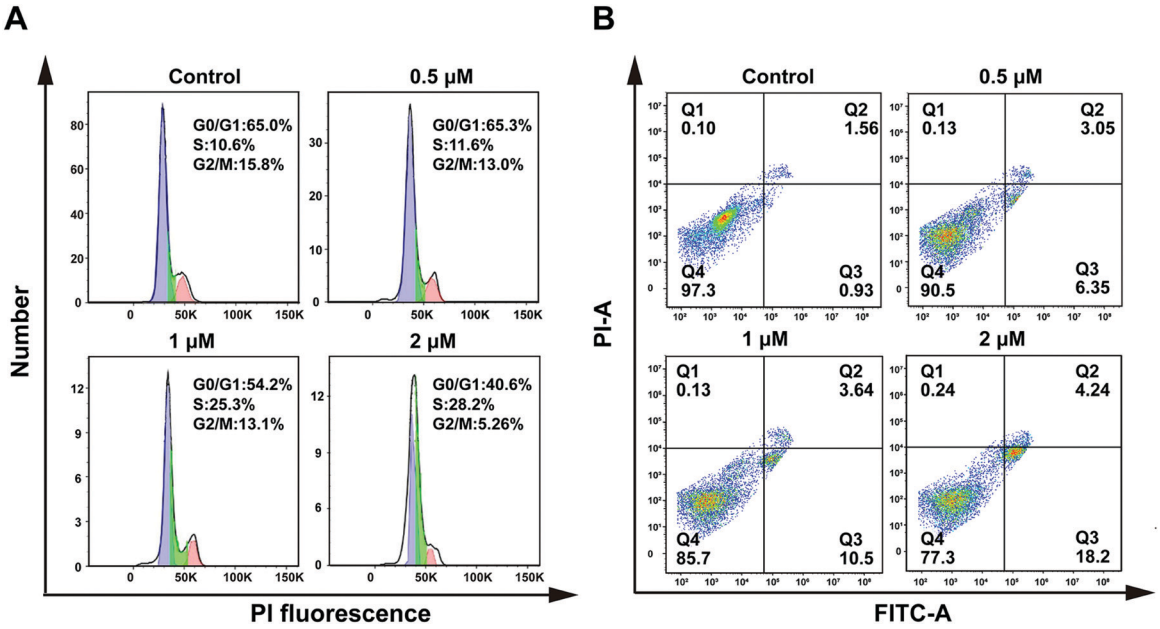

Fig. 6 Cell cycle distributions (A) and apoptosis analysis (B) of HeLa cells treated with **EDY-E** of indicated concentrations.

γ-H2AX foci induced by DNA damage. The higher level of γ-H2AX represents a much deeper degree of DNA damage.[57] As shown in Fig. 5C, While the expression of γ-H2AX (red color) in the nuclei (blue color) is not observed in the control groups, cells treated with either **EDY-E** or **EDY-F** exhibit significant levels of γ-H2AX foci. These studies further illustrate that the cytotoxicity of enediynes mainly originates from DNA damage.

Cell cycle arrest and apoptosis induced by enediynes

Intracellular DNA damage induced by radicals or ROS may disrupt the cell cycle distribution, thereby inducing cell death *via* an apoptosis pathway. Herein, HeLa cells were cultured with varied concentrations of **EDY-E** for 8 h, and the cell cycle distribution and apoptosis were detected by flow cytometry. As shown in Fig. 6A and Fig. S7 (ESI†), **EDY-E** causes the extension of the S phase from 10.6% to 28.2%, accompanied by a decrease in the G2/M phase in a dose-dependent manner, indicating that the cells are arrested at the S phase, which is in line with our previous reports.[20,22] Blocking the cell cycle at the S phase suggests that **EDY-E** may display its cytotoxicity through the inhibition of DNA replication. In addition, Fig. 6B and Fig. S8 (ESI†) show that **EDY-E** mainly induced cell death *via* an apoptosis pathway in a dose-dependent manner. These results confirmed that the diradicals generated from enediynes effectively disrupted the distribution of cell cycles and promoted the generation of apoptotic signals, thereby generating a toxic effect on tumor cells.

Conclusions

In summary, several maleimide-based enediynes were synthesized by varying the introduction and position of cyclopropane moieties. The radical clock reaction through ring-opening of cyclopropane moieties was confirmed to generate a new diradical species with two radical sites being separated faraway, enhancing their radical character and H-abstracting reactivity. The enediynes with cyclopropane moieties showed higher DNA-cleavage efficiency and cytotoxicity toward HeLa cell lines. In addition, these maleimide-based enediynes showed unaffected cytotoxicity under hypoxia conditions, providing a promising way for cancer treatment in solid tumors. Further studies indicated that enediynes disrupted the distribution of cell cycles through intracellular DNA damage, thereby inducing cell death *via* an apoptosis pathway. Overall, cyclopropane substituted maleimide-based enediynes having a potential radical clock pathway can be potentially used as efficient antitumor agents for cancer chemotherapy.

Conflicts of interest

There are no conflicts to declare.

Acknowledgements

Dedicated to the 100th anniversary of Chemistry at Nankai University. The authors gratefully acknowledge the financial support from the National Natural Science Foundation of China (21871080, 21503078, 21474027), the Fundamental Research Funds for the Central Universities (22221818014), and the Shanghai Leading Academic Discipline Project (B502). AH acknowledges the ''Eastern Scholar Professorship'' support from Shanghai local government.

Notes and references

1 N. Ishida, K. Miyazaki, K. Kumagai and M. Rikimaru, *J. Antibiot., Ser. A*, 1965, **18**, 68–76.
2 T. Nishikawa, K. Kumagai, A. Kudo and N. Ishida, *J. Antibiot.*, 1965, **18**, 223–227.
3 M. D. Lee, T. S. Dunne, C. C. Chang, M. M. Siegel, G. O. Morton, G. A. Ellestad, W. J. McGahren and D. B. Borders, *J. Am. Chem. Soc.*, 1992, **114**, 985–997.
4 M. Konishi, H. Ohkuma, K. Matsumoto, T. Tsuno, H. Kamei, T. Miyaki, T. Oki, H. Kawaguchi, G. D. Vanduyne and J. Clardy, *J. Antibiot.*, 1989, **42**, 1449–1452.
5 J. Golik, J. Clardy, G. Dubay, G. Groenewold, H. Kawaguchi, M. Konishi, B. Krishnan, H. Ohkuma, K. Saitoh and T. W. Doyle, *J. Am. Chem. Soc.*, 1987, **109**, 3461–3462.
6 A. L. Smith and K. Nicolaou, *J. Med. Chem.*, 1996, **39**, 2103–2117.
7 K. C. Nicolaou and W. M. Dai, *Angew. Chem., Int. Ed. Engl.*, 1991, **30**, 1387–1416.
8 K. C. Nicolaou, W.-M. Dai, S.-C. Tsay, V. A. Estevez and W. Wrasidlo, *Science*, 1992, **256**, 1172–1178.
9 K. C. Nicolaou, Z. Lu, R. Li, J. R. Woods and T.-i. Sohn, *J. Am. Chem. Soc.*, 2015, **137**, 8716–8719.
10 K. C. Nicolaou, Y. Wang, M. Lu, D. Mandal, M. R. Pattanayak, R. Yu, A. A. Shah, J. S. Chen, H. Zhang, J. J. Crawford, L. Pasunoori, Y. B. Poudel, N. S. Chowdari, C. Pan, A. Nazeer, S. Gangwar, G. Vite and E. N. Pitsinos, *J. Am. Chem. Soc.*, 2016, **138**, 8235–8246.
11 K. C. Nicolaou, E. P. Schreiner, Y. Iwabuchi and T. Suzuki, *Angew. Chem., Int. Ed. Engl.*, 1992, **31**, 340–342.
12 K. C. Nicolaou and A. L. Smith, *Acc. Chem. Res.*, 1992, **25**, 497–503.
13 A. G. Myers, *Tetrahedron Lett.*, 1987, **28**, 4493–4496.
14 G. dos Passos Gomes and I. V. Alabugin, *J. Am. Chem. Soc.*, 2017, **139**, 3406–3416.
15 R. Romeo, S. V. Giofre and M. A. Chiacchio, *Curr. Med. Chem.*, 2017, **24**, 3433–3484.
16 R. K. Mohamed, P. W. Peterson and I. V. Alabugin, *Chem. Rev.*, 2013, **113**, 7089–7129.
17 J. W. Grissom and D. Huang, *J. Org. Chem.*, 1994, **59**, 5114–5116.
18 E. Rettenmeier, M. M. Hansmann, A. Ahrens, K. Rübenacker, T. Saboo, J. Massholder, C. Meier, M. Rudolph, F. Rominger and A. S. K. Hashmi, *Chem. – Eur. J.*, 2015, **21**, 14401–14409.
19 A. V. Kuzmin and V. V. Popik, *Chem. Commun.*, 2009, 5707–5709.
20 M. Zhang, B. Li, H. Chen, H. Lu, H. Ma, X. Cheng, W. Wang, Y. Wang, Y. Ding and A. Hu, *J. Org. Chem.*, 2020, **85**, 9808–9819.
21 Y. Wang, B. Li, M. Zhang, H. Lu, H. Chen, W. Wang, Y. Ding and A. Hu, *Tetrahedron*, 2020, **76**, 131242.
22 H. Lu, H. Ma, B. Li, M. Zhang, H. Chen, Y. Wang, X. Li, Y. Ding and A. Hu, *J. Mater. Chem. B*, 2020, **8**, 1971–1979.
23 M. E. Cremeens, T. S. Hughes and B. K. Carpenter, *J. Am. Chem. Soc.*, 2005, **127**, 6652–6661.
24 P. W. Peterson, R. K. Mohamed and I. V. Alabugin, *Eur. J. Org. Chem.*, 2013, 2505–2527.
25 A. G. Myers, P. S. Dragovich and E. Y. Kuo, *J. Am. Chem. Soc.*, 1992, **114**, 9369–9386.
26 H. Sugiyama, K. Yamashita, T. Fujiwara and I. Saito, *Tetrahedron*, 1994, **50**, 1311–1325.
27 I. Suzuki, M. Wakayama, A. Shigenaga, H. Nemoto and M. Shibuya, *Tetrahedron Lett.*, 2000, **41**, 10019–10023.
28 T. P. Goncalves, M. Mohamed, R. J. Whitby, H. F. Sneddon and D. C. Harrowven, *Angew. Chem., Int. Ed.*, 2015, **54**, 4531–4534.
29 P. G. Wenthold and A. H. Winter, *J. Org. Chem.*, 2018, **83**, 12397–12403.
30 D. C. Ding, H. N. Jiang, X. Ma, J. J. Nash and H. I. Kenttamaa, *J. Org. Chem.*, 2020, **85**, 8415–8428.
31 G. Bucher, A. A. Mahajan and M. Schmittel, *J. Org. Chem.*, 2009, **74**, 5850–5860.
32 W. M. Kincannon, N. A. Bruender and V. Bandarian, *Biochemistry*, 2018, **57**, 4816–4823.
33 Y. Mai-Linde and T. Linker, *Org. Lett.*, 2020, **22**, 1525–1529.
34 M. Schmittel, A. A. Mahajan, G. Bucher and J. W. Bats, *J. Org. Chem.*, 2007, **72**, 2166–2173.
35 H.-N. Shi, M.-H. Huang, C.-L. He, H.-P. Lu, W.-J. Hao, X.-C. Tu, S.-J. Tu and B. Jiang, *J. Org. Chem.*, 2019, **84**, 13686–13695.
36 P. G. Dopico and M. G. Finn, *Tetrahedron*, 1999, **55**, 29–62.
37 H. Chen, B. Li, M. Zhang, H. Lu, Y. Wang, W. Wang, Y. Ding and A. Hu, *ChemistrySelect*, 2020, **5**, 7069–7075.
38 H. Lu, M. Zhang, B. Li, H. Ma, W. Wang, Y. Ding, X. Li and A. Hu, *Asian J. Org. Chem.*, 2020, **9**, 2170–2175.
39 M. Zhang, H. Lu, B. Li, H. Ma, W. Wang, X. Cheng, Y. Ding and A. Hu, *J. Org. Chem.*, 2021, **86**, 1549–1559.
40 R. Frlan, M. Sova, S. Gobec, G. Stavber and Z. Casar, *J. Org. Chem.*, 2015, **80**, 7803–7809.
41 R. Kancherla, K. Muralirajan, B. Maity, C. Zhu, P. E. Krach, L. Cavallo and M. Rueping, *Angew. Chem., Int. Ed.*, 2019, **58**, 3412–3416.
42 E. G. Janzen and B. J. Blackburn, *J. Am. Chem. Soc.*, 1968, **90**, 5909–5910.
43 Z. Zhao, Y. Han, C. Lin, D. Hu, F. Wang, X. Chen, Z. Chen and N. Zheng, *Chem. – Asian J.*, 2012, **7**, 830–837.
44 D. Song, S. Sun, Y. Tian, S. Huang, Y. Ding, Y. Yuan and A. Hu, *J. Mater. Chem. B*, 2015, **3**, 3195–3200.
45 J. Li, B. Li, L. Sun, B. Duan, S. Huang, Y. Yuan, Y. Ding and A. Hu, *J. Mater. Chem. B*, 2019, **7**, 103–111.
46 P. Huang, D. Wang, Y. Su, W. Huang, Y. Zhou, D. Cui, X. Zhu and D. Yan, *J. Am. Chem. Soc.*, 2014, **136**, 11748–11756.
47 Z. Dong, J. Z. Wang, F. Yu and M. A. Venkatachalam, *Am. J. Pathol.*, 2003, **163**, 663–671.
48 J. Zhou, T. Schmid, S. Schnitzer and B. Brüne, *Cancer Lett.*, 2006, **237**, 10–21.
49 C. Jean-Philippe and M. Carine, *Anti-Cancer Agents Med. Chem.*, 2008, **8**, 790–797.

50 Y. Wan, G. Lu, J. Zhang, Z. Wang, X. Li, R. Chen, X. Cui, Z. Huang, Y. Xiao, J. Chelora, W. Zhang, Y. Liu, M. Li, H. Y. Xie and C. S. Lee, *Adv. Funct. Mater.*, 2019, **29**, 1903436.
51 X. Li, Y. Wei, Y. Wu and L. Yin, *Angew. Chem., Int. Ed.*, 2020, **59**, 22544–22553.
52 A. A. Almaqwashi, W. Zhou, M. N. Naufer, I. A. Riddell, O. H. Yilmaz, S. J. Lippard and M. C. Williams, *J. Am. Chem. Soc.*, 2019, **141**, 1537–1545.
53 P.-F. Zhao, A. Liu, M.-G. Wei and Z.-Q. Liu, *J. Org. Chem.*, 2019, **84**, 15854–15864.
54 Y. Gilad and H. Senderowitz, *J. Chem. Inf. Model.*, 2014, **54**, 96–107.
55 G. M. Morris, R. Huey, W. Lindstrom, M. F. Sanner, R. K. Belew, D. S. Goodsell and A. J. Olson, *J. Comput. Chem.*, 2009, **30**, 2785–2791.
56 T. Tuttle, E. Kraka and D. Cremer, *J. Am. Chem. Soc.*, 2005, **127**, 9469–9484.
57 Y. V. Surovtseva, V. Jairam, A. F. Salem, R. K. Sundaram, R. S. Bindra and S. B. Herzon, *J. Am. Chem. Soc.*, 2016, **138**, 3844–3855.